2014 IEEE International Conference on Robotics & Automation (ICRA)
Hong Kong Convention and Exhibition Center
May 31 - June 7, 2014. Hong Kong, China

A Haptic Human-Robot Interface Accounting for Human Parameter Stochasticity

William Gallagher Jun Ueda

***Abstract*— Force feedback haptic devices require physical contact between the operator and the machine, creating a coupled system where the stiffness changes based on that of the operator's arm. The natural human tendency to increase arm stiffness to stabilize motion increases the overall stiffness and reduces stability. Controllers commonly address this with increased damping, which slows the device and decreases operator efficiency. Previous research designed a system to estimate operator arm stiffness by measuring muscle activity and compensate accordingly, modifying the robot's motion based on operator interactions. This achieved the goal of reducing oscillations and increasing performance, but encountered drawbacks related to the unpredictable way in which humans modulate the dynamic parameters of their arm. Controllers designed to be robust to stochastic variation of system parameters are explored, and their effectiveness is validated experimentally. This could further increase the operator performance and reduce fatigue, which could translate into better efficiency and higher productivity.**

I. Introduction

As robotic technology advances, the area of human-robot interaction (HRI) is expanding rapidly. Robots can no longer be designed in isolation from the people that will use them, as typical industrial systems have been. HRI systems must consider that the human is an integral part of the system. This applies especially to physical human-robot interaction (pHRI) systems, where the operator is in physical contact with the robot. Contact between the robot and the human gives a coupled system, requiring a design incorporating an understanding of how the human will move.

Industrial settings are increasingly utilizing robotics and automation to streamline difficult jobs, but some situations make automation difficult due to the usually strict tolerances required for repetitive tasks. For exampe, on vehicle assembly lines, the placement of a vehicle component, such as a door, must be done within tolerances, but the location of the vehicle itself may vary slightly. It is often more efficient to have a human accomplish the task, especially for ones that requires a cautious force sensitivity that is best accomplished through human touch. Components can often be heavier than a worker can lift, but assistive robotic devices can be useful in aiding the completion of such tasks through force amplification. Teleoperated systems could be used, but this removes the operator from directly participating in the task through remote sensing, introducing possible errors and requiring slower motion. A system that the operator could directly interact with is preferred.

Haptics is a popular control method, since people find touch very intuitive for controlling a robotic device. Force feedback and haptic controllers are common from gaming to industrial machines. Physical contact between the operator and robot introduces force feedback, creating a coupled operator-robot system. This can result in reduced stability without an appropriate controller, making the robot harder to operate. Instability increases task completion time, decreases performance, and creates an opportunity for injury. Humans naturally increase muscle stiffness to control to instability or oscillation. Unfortunately, this creates a stiffer coupled system with more instability. Generic robot controllers cannot directly measure or adjust to operator stiffness. A system with access to information about the operator's motion could adjust accordingly, and thereby increase stability, bolster safety, and make operation easier. This would enable increased operator performance, which in industrial settings can result in increased efficiency.

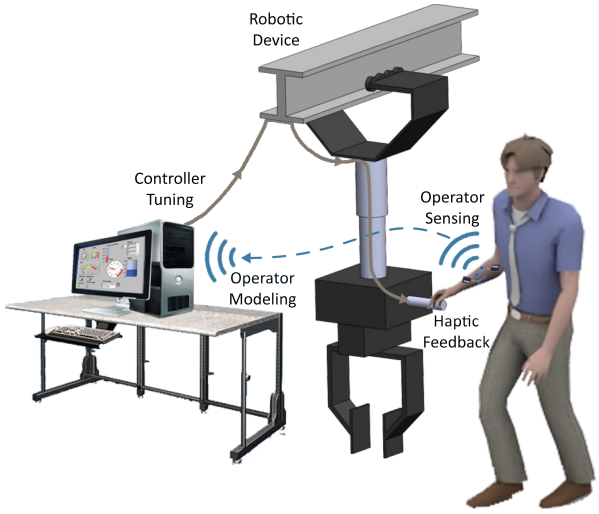

Fig. 1. Conceptual drawing of a haptically controlled robotic device with a controller that adjusts based on estimated operator model

This research developed a method to allow a haptic robot controller to adjust to changes in how the operator interacts with the robot by expanding the information available to the controller. Fig 1 shows a conceptual illustration of the system. It will measure metrics indicative of how the operator intends to move the device and incorporate them into a model to estimate the operator's current motion. The controller then adjusts its gains to assist. This allows the robot to actively adjust to changes in the operator's motion, ensuring stability and ease of use. While it may be possible to instead design a robust system to accommodate a wider range of parameters, this tends to result in lower performance, which is counter to the requirements of industrial settings.

Bio-Robotics and Human Modling Lab, Woodruff School of Mechanical Engineering, Georgia Institute of Technology, Atlanta, GA, USA

978-1-4799-3684-7/14/$31.00 ©2014 IEEE

II. Background

A. Haptic Assist Systems

Early work on force amplifying assistive devices by Kazerooni led to the design of a force amplifying exoskeleton system [1, 2]. Li has also investigated force amplification control for industrial type robots, which allow an operator to manipulate heavy loads [3]. Such systems commonly use impedance control, which masks the physical system dynamics by generating an assistive force so the operator feels some desired system dynamics [4].

Impedance based control methods can be effective in increasing stability [5]. Limitations on how people adapt to rapid changes in dynamics create a design trade off between high performance and stability [6]. People modulate their arm motion to help control unstable dynamics [7], leading to work on how to measure the dynamic characteristics of the arm effictively [8]. Compensating systems have been demonstrated to be capable of increased stability without sacrificing performance [9].

B. Human Arm Stiffness

Muscles can be modeled primarily as springs, though nonlinear effects exist [10–12]. There is a reflexive component of the nervous system's attempts to maintain muscle length which introduces a delay [13]. Generally, a larger muscle force will exhibit a higher stiffness. Increases in joint stiffness have been linked to simultaneous activation of antagonistic muscles, or cocontraction [14], which causes an increase in end-point stiffness [5], making cocontraction of primary interest. People generally can not control end-point stiffness independently of force and position [15], which implies that an estimate of end-point stiffness is indicative of upcoming motion. For consistent pose and low velocities, a simplified linear stiffness model can be assumed [16], modeling the arm as a mass-spring-damper system attached to the robot handle [17]. People correct for variations from a desired motion by increasing arm stiffness, leading to increased cocontraction [18, 19].

III. Stiffness Compensating System

Prior work designed and tested a system that modeled arm stiffness, k_o, and adjusted an impedance controller accordingly, as represented by Fig 2. Stiffness was estimated from muscle activity measured by electromyogram (EMG). Feasibility testing with volunteers measured its effect on stability and performance. Ultimately, this should lead to an industrially viable way of making robot operation easier, and could be used in various human-machine interfaces with applications such as industrial assembly lines, rehabilitaiton robotics, or space robots. Further details not presented here are in [20–23].

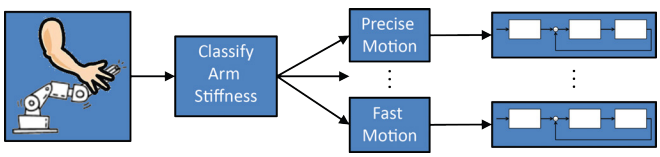

Fig. 2. Basic tasks of compensating system

A. Estimating Arm Stiffness

The Biceps Brachii (BB) and Triceps Brachii (TB) at the elbow (E) and the Extensor Carpi Ulnaris (ECU) and Flexor Carpi Ulnaris (FCU) at the wrist (W) were chosen as the best muscles for measuring cocontraction, CC_i, $i = E, W$, with EMG. A threshold based classifier was developed, which determined based on the two cocontraction levels if the stiffness level, Z, was high or low using the thresholds ℓ_W & ℓ_E as per (1).

$$Z = \begin{cases} high & \text{if } CC_W(t) \geq \ell_W \text{ or } CC_E(t) \geq \ell_E \\ low & \text{if } CC_W(t) < \ell_W \text{ and } CC_E(t) < \ell_E \end{cases} \quad (1)$$

Testing showed that more than two levels provided no statistically significant advantage, as shown by Fig 3. Further, the data showed that the stiffness level generated by operators was inconsistent and not necessarily just high enough for the applied force. The stiffness, k_o, data collected was poorly fit by several common distributions, but proved to be well fit by two separate Gaussians, shown in Fig 4, supporting the two level classification scheme.

B. Adjusting Controller

An impedance controller calculated the control force so that the operator felt the dynamics of some desired model system with mass, m_d, damping, b_d, and stiffness, k_d. This consised of an outer force component that passed this motion to an inner position component utilizing a PD controller with gains K_p and K_d. Fig 5 gives the complete system, where m, b, and k are mass, damping, and stiffness, with the subscripts

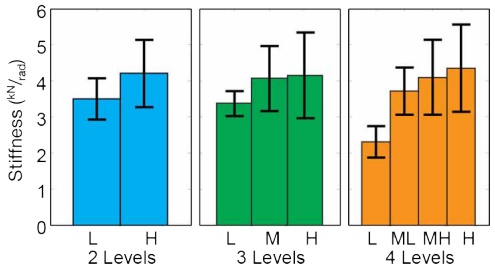

Fig. 3. Average of classified stiffness levels for experimental data, error bars show standard deviation of classified points.

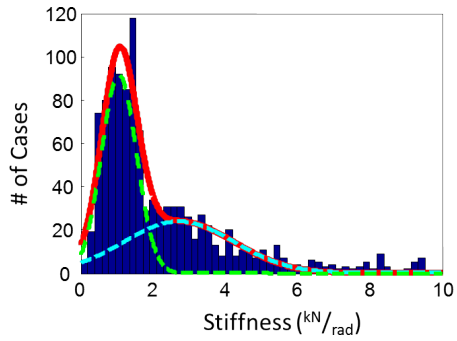

Fig. 4. Stiffness, k_o, data fit with two normal distributions, $R^2 = 0.917$

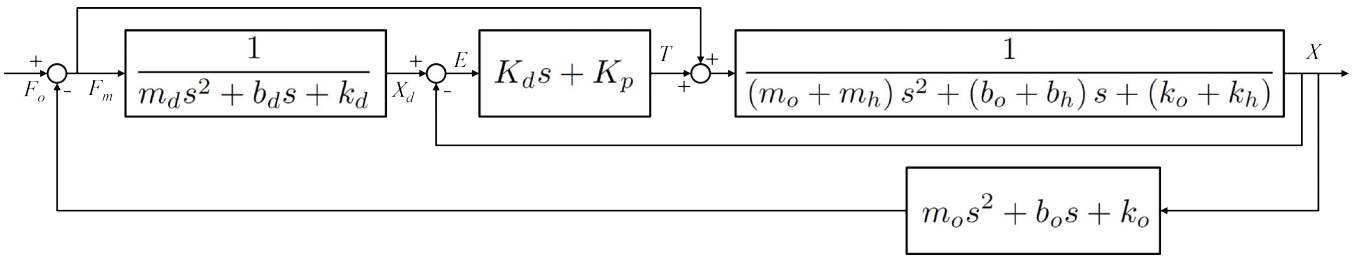

Fig. 5. s domain block diagram of impedance controller utilizing PD inner position control and operator system, as designed in [20–22]. Laplace domain variables - F_o: Operator applied force, F_m: Measured force, X_d: Desired position, E: Position error, T: Motor torque, X: Position

d, h, and o, denoting desired impedance characteristics of the controller, dynamics of the haptic device, and dynamics of the operator, respectively. Human contact decreased its stability, especially when the operator stiffness, k_o, increased, therefore the desired values were adjusted based on the classified stiffness. Experiments validated that stability increased as compared to a fixed system with the same performance capability. Additionally, it provided better performance that the typical more stable system.

However, there was a large amount of chatter in the system, where the compensation would turn on and off rapidly, which reduced performance and is undesireable. This stemmed from the non-deterministic nature of the operator stiffness, so tolerance of stochastically varying parameters would be better. This research proposes replacing the PD controller with an optimal controller designed to account for the stochastic changes in human arm dynamics.

IV. Control of Stochastic Systems

Humans do not deterministically generate force or stiffness for the task they are performing. Since the complete system is coupled between the human and device, the overall system dynamics are changing in an unknown and stochastic manner. Therefore, it is desirable for the controller to be tolerant of these variances in the system parameters.

Consider the state space representation of the system given by (2), where the system input, u is the applied force.

$$\dot{x} = \boldsymbol{A}x + \boldsymbol{B}u \qquad y = \boldsymbol{C}x + \boldsymbol{D}u \tag{2}$$

where $\boldsymbol{A} = \begin{bmatrix} 0 & 1 \\ -\frac{k_o+k_h}{m_h} & -\frac{b_o+b_h}{m_h} \end{bmatrix}$, $\boldsymbol{B} = \begin{bmatrix} 0 \\ \frac{1}{m_h} \end{bmatrix}$, $\boldsymbol{C} = \begin{bmatrix} 1 & 0 \end{bmatrix}$, and $\boldsymbol{D} = 0$. The $\boldsymbol{A}$ matrix varies stochastically as the dynamic parameters of the arm, k_o and b_o, change. A controller designed for uncertain system parameters can minimize the effect of these variations and can be substituted for inner PD position controller in the impedance control scheme of Fig 5. An expected distribution of operator arm stiffness can be found experimentally, allowing the design of a controller that is optimal for the expected range of values.

A. Linear Quadratic Gaussian Control

The Linear Quadratic Regulator (LQR) is a common optimal controller designed to stabilize a system with minimum control effort [24], relying on the assumption that the system is time-invariant. It can be adapted to control stochastic systems by modeling variation as additive or multiplicative noise [25]. Combined with Kalman's filter to reduce uncertainty and noise [26], the Linear Quadratic Gaussian (LQG) control method is obtained [27], which has become one of the fundamental techniques for control under uncertainty.

Consider a discrete linear system given by (3), where the system matrices $\boldsymbol{A}$, $\boldsymbol{B}$, and $\boldsymbol{C}$ are assumed time-invariant.

$$x_{t+1} = \boldsymbol{A}x_t + \boldsymbol{B}u_t \qquad y_t = \boldsymbol{C}x_t \tag{3}$$

The LQR optimal control input, $u_0, u_1, ..., u_t$, is found by (4), where $\boldsymbol{L}$ is derived via the minimization of the cost function, J, in (5) for all t. $\boldsymbol{Q}_1$ and $\boldsymbol{Q}_2$ are weighting matrices to emphasize minimization of error and control effort, respectively, and are positive semi-definite.

$$u_t = -\boldsymbol{L}x_t \tag{4}$$

$$J = \sum_{t=0}^{\infty} \left(x_t^\top \boldsymbol{Q}_1 x_t + u_t^\top \boldsymbol{Q}_2 u_t \right) \tag{5}$$

The solution by dynamic programming porvides the Ricatti equation in (6), giving the optimal control law in (7).

$$\boldsymbol{\Phi} = \boldsymbol{Q}_1 + \boldsymbol{A}^\top \boldsymbol{\Phi} \boldsymbol{A} - \boldsymbol{A}^\top \boldsymbol{\Phi} \boldsymbol{B} \left(\boldsymbol{Q}_2 + \boldsymbol{B}^\top \boldsymbol{\Phi} \boldsymbol{B} \right)^{-1} \boldsymbol{B}^\top \boldsymbol{\Phi} \boldsymbol{A} \tag{6}$$

$$\boldsymbol{L} = \left(\boldsymbol{Q}_2 + \boldsymbol{B}^\top \boldsymbol{\Phi} \boldsymbol{B} \right)^{-1} \boldsymbol{B}^\top \boldsymbol{\Phi} \boldsymbol{A} \tag{7}$$

This solution is optimal and minimizes control effort. However, it relies on the accuracy of the system model and the assumption of time invariance. Consider, instead, the system with sensor output given by (8), where v_t is process noise and w_t is sensor noise.

$$x_{t+1} = \boldsymbol{A}x_t + \boldsymbol{B}u_t + v_t \qquad y_t = \boldsymbol{C}x_t + w_t \tag{8}$$

The process and sensor noise are unknowable a priori and not directly measurable. Utilizing the Kalman filter in (9) to perform state estimation provides more accurate values for the control law, given in (10).

$$\hat{x}_{t+1} = \boldsymbol{A}\hat{x}_t + \boldsymbol{B}u_t + \boldsymbol{K} \left(y_{t+1} - \boldsymbol{C} \left(\boldsymbol{A}\hat{x}_t + \boldsymbol{B}u_t \right) \right) \tag{9}$$

$$u_t = -\boldsymbol{L}\hat{x}_t \tag{10}$$

The $\boldsymbol{K}$ found from the Ricatti equation in (11) and control law solution in (12) is combined with the $\boldsymbol{L}$ found previously. The diagonals of $\boldsymbol{W}$ and $\boldsymbol{V}$ give the expected range of the elements of w_t and v_t, respectively.

$$\boldsymbol{\Gamma} = \boldsymbol{V} + \boldsymbol{A}\boldsymbol{\Gamma}\boldsymbol{A}^\top - \boldsymbol{A}\boldsymbol{\Gamma}\boldsymbol{C}^\top \left(\boldsymbol{W} + \boldsymbol{C}\boldsymbol{P}\boldsymbol{C}^\top \right)^{-1} \boldsymbol{C}\boldsymbol{\Gamma}\boldsymbol{A}^\top \tag{11}$$

$$\boldsymbol{K} = \boldsymbol{\Gamma}\boldsymbol{C}^\top \left(\boldsymbol{W} + \boldsymbol{C}\boldsymbol{\Gamma}\boldsymbol{C} \right)^{-1} \tag{12}$$

A diagram of the LQG controller is shown in Fig 6.

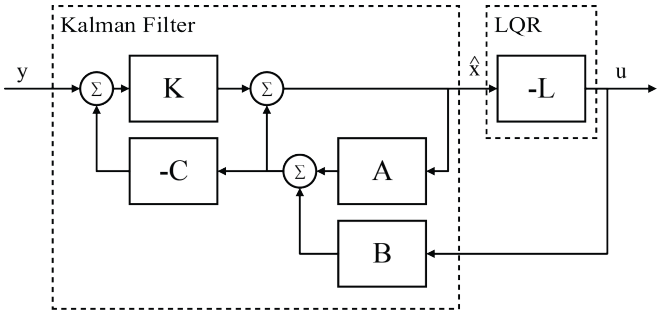

Fig. 6. State feedback block diagram of LQG controller

B. LQR for Stochastically Varying Parameters

The LQG controller is not designed specifically for systems with parameters that vary stochastically, but for time invariant systems disturbed by noise. Minimax LQG controllers handle complex uncertainty [28], but rely on an assumption of bounded noise rather than a direct change in system parameters. Controllers that attempt to minize Kullback-Leibler distance [29] or the H_∞ norm of the system rather than a control cost function [30] exist, but often focused on fixed dynamics with unknown time delay. The most promising of these approaches for this research incorporated an assumed distribution for the system parameters directly into the derivation of the optimal control law, ensuring that the controller was optimal for their expected value, but still perform well as they varied [31, 32].

Consider (3) where $\boldsymbol{A}$ and $\boldsymbol{B}$ have expected values $\mathrm{E}[\boldsymbol{A}]$ and $\mathrm{E}[\boldsymbol{B}]$ vary stochastically according to some distribution that does not change with time. The cost function should therefore minimize not only the control effort, but also the variance of the system's error, as in (IV-B).

$$J = \mathrm{E}\left[\sum_{t=0}^{\infty}\left(x_t^\top \boldsymbol{Q}_1 x_t + u_t^\top \boldsymbol{Q}_2 u_t + \mathrm{tr}\left[\boldsymbol{Q}_3 \mathrm{cov}\left[x_{t+1}, x_t\right]\right]\right)\right] \tag{13}$$

By the methodology of Fujimoto [31, 32], the optimal control gain is found by (16), with the parameter $\boldsymbol{\Pi}$ given by (IV-B) and the covariances $\boldsymbol{\Sigma}_{XY}$ given by (15).

$$\boldsymbol{\Pi} = \boldsymbol{Q}_1 + \boldsymbol{\Sigma}_{AA} + \mathrm{E}\left[\boldsymbol{A}^\top \boldsymbol{\Pi} \boldsymbol{A}\right] - \left(\mathrm{E}\left[\boldsymbol{A}^\top \boldsymbol{\Pi} \boldsymbol{B}\right] + \boldsymbol{\Sigma}_{AB}\right) \left(\mathrm{E}\left[\boldsymbol{B}^\top \boldsymbol{\Pi} \boldsymbol{B}\right] + \boldsymbol{\Sigma}_{BB} + \boldsymbol{Q}_2\right)^{-1} \left(\mathrm{E}\left[\boldsymbol{B}^\top \boldsymbol{\Pi} \boldsymbol{A}\right] + \boldsymbol{\Sigma}_{BA}\right) \tag{14}$$

$$\boldsymbol{\Sigma}_{XY} = \mathrm{E}\left[\boldsymbol{X}^\top \boldsymbol{Q}_3 \boldsymbol{Y}\right] - \mathrm{E}\left[\boldsymbol{X}\right]^\top \boldsymbol{Q}_3 \mathrm{E}\left[\boldsymbol{Y}\right] \tag{15}$$

$$\boldsymbol{L} = \left(\mathrm{E}\left[\boldsymbol{B}^\top \boldsymbol{\Pi} \boldsymbol{B}\right] + \boldsymbol{\Sigma}_{BB} + \boldsymbol{Q}_2\right)^{-1} \left(\mathrm{E}\left[\boldsymbol{B}^\top \boldsymbol{\Pi} \boldsymbol{A}\right] + \boldsymbol{\Sigma}_{BA}\right) \tag{16}$$

This Stochastic Linear Quadratic Regulator (SLQR), shown by Fig 7, is an optimal controller designed from the expected value and covariance of $\boldsymbol{A}$ and $\boldsymbol{B}$ to minimize the control effort and variance of the system. The emphasis on each of these can be varied by choosing appropriate values for the $\boldsymbol{Q}$'s. The state feedback diagram is drastically simpler, as the state estimator is removed, since the calculation of $\boldsymbol{L}$ already incorporates an estimate of the stochasticity of the system.

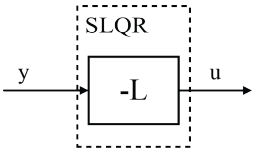

Fig. 7. State feedback block diagram of SLQR controller

V. Experimental Validation

A. Concept

The stochastic controllers were incorporated into the system, replacing the PD position component of the impedance controller and tested against each other and the baseline system to evaluated the effects on system performance. The compensating system was also compared with fixed gain systems with high damping for stability or low damping for speed. It was expected that the compensation would give better performance than current fixed high damping systems with regards to speed while providing better accuracy than fixed low damping systems.

Two tasks were designed to allow targeted testing of speed and accuracy. In each task, the participant was given a series of targets to reach on a computer screen in front of the device. For the speed-based task, participants were told to move the indicator to the target as quickly as possible, with overshoot acceptable. For the accuracy-based task, they were told to move the indicator to the target as accurately as possible and to avoid overshoot. For both tasks, the operator was given a score for each target that was displayed once they had reached the target. The simulation, shown in Fig 8, characterized accuracy and speed improvements independently in a rigorous fashion.

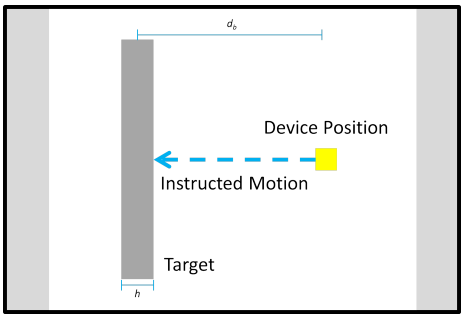

Fig. 8. Experimental simulation - Yellow box moved with device handle; Gray box was target with an emphasis on either speed or accuracy

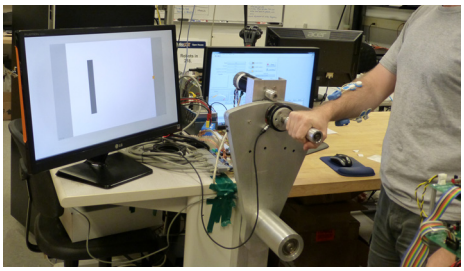

Fig. 9. A participant performing the experiment

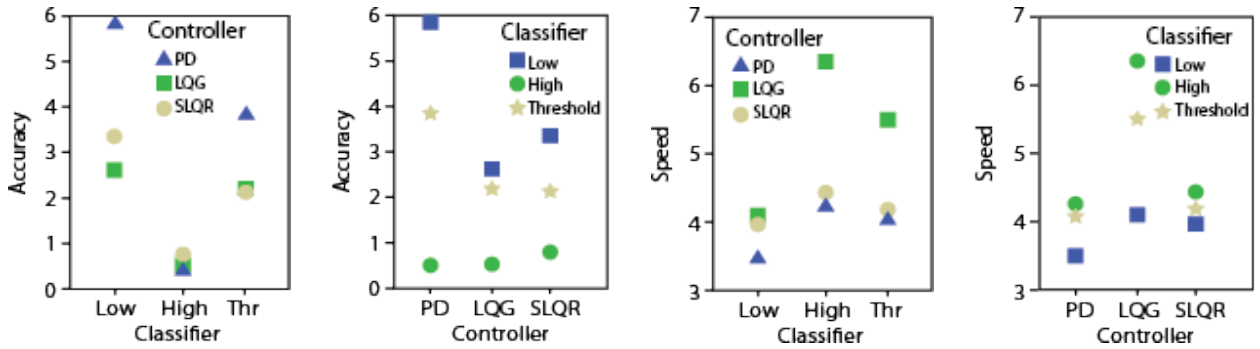

(a) Accuracy task by classifier (b) Accuracy task by controller (c) Speed task by classifier (d) Speed task by controller

Fig. 10. Performance comparison experiment marginal means, lower scores indicate better performance

TABLE I
PERFORMANCE COMPARISON PARTICIPANT DATA

Total	Male	Female	Ages
24	16	8	19 - 42

B. Method

The experiment utilized a one degree of freedom haptic paddle system, which was used previous for system design and testing, and is described further in [20–22]. The 1-DOF device can be seen in Fig 9, which shows a participant with the simulation displayed on the screen in front of them.

Participants stood next to the device with their right elbow bent approximately $90°$, grasping the handle with the right hand, with EMG sensors attached to the four muscles of their right arm They were given the instructions for each task and allowed to run practice trials.

Each participant performed a full factorial of cases, with 3 classifiers and 3 controllers for both tasks, giving 18 trials, each of which consisted of 24 scored targets. The trials were ordered based on a Latin Squares design to esnure that each participant saw the tasks in a unique order and to minimize the effects of learning and fatigue. This was conducted following an approved IRB protocol.

C. Analysis

The experiment included data from 24 volunteers, given in Tbl I. Over 10,000 data points were collected, with a statistical power of $1-\beta > 0.999$, ensuring strong statistical significance. The analysis utilized a generalized linear model to perform a repeated-measures multivariate ANOVA.

The speed task score, j_s, given by (17), normalized time to the target, t_b, by the distance to the target, d_b. Equal scores were differentiated with an accuracy factor based on overshoot time, t_o. A lower score indicated better performance.

$$j_s = \frac{t_b}{d_b} + c_s t_s \tag{17}$$

The accuracy task score, j_a, given by (18), was closest distance to the target reached, d_{min}, normalized by the target width, h, and squared to more strongly penalize poor accuracy. Overshoot was penalized by replacing d_{min} with the maximum overshoot, d_s, and adding an additional penalizing factor was added. Equal scores were differentiated with a time factor accounting for the velocity to reach the target, $\dot{x}_z$. A lower score indicated better performance.

$$j_a = \begin{cases} \left(\frac{d_{min}}{h}\right)^2 - \frac{\dot{x}_b}{\dot{x}_{max}} & \text{if no overshoot} \\ \left(\frac{d_s}{h}\right)^2 + \frac{d_s}{h} + \frac{\dot{x}_b}{\dot{x}_{max}} & \text{if overshoot} \end{cases} \tag{18}$$

D. Results

Fig 10 shows the means of the data for both tasks, separated by classifier in Figs 10(c) and 10(a) and by controller in Figs 10(d) and 10(b), with all differences proving statistically significant. All statistics presented are corrected F value using Pillai's trace, and, unless otherwise stated, $p < 0.001$ may be assumed.

Results demonstrated that the classifier had a statistically significant effect on both tests, with $PV = 0.112$ and $F = 162.0$. The controller's effect was also statistically significant, with $PV = 0.125$ and $F = 273.9$. Interactions between the two independent variables proved to have a statistically significant effect, with $PV = 0.48$ and $F = 33.52$.

Pairwise comparisons between each of the classifiers showed statistically significance differences with $p < 0.001$. Between the controllers, all pairs were significantly different with $p < 0.001$, except for between the LQG and SLQR, which showed significance with $p = 0.017$.

E. Discussion

The results strongly suggest improvement over the non-compensating system. The trade-off between the speed achieved with low damping and accuracy achieved with high damping is clearly demonstrated, with the compensating system achieving a balance between the two.

The low damping case provided the worst accuracy scores and the high damping case provided the best. Fig 10(a) the improved accuracy of compensating system over the low damping case, especially with a stochastic controller. Statistically, there is little difference between the LQG and SLQR controllers, but the SLQR performed better with the compensating system. In all cases except for the high damping case, the two stochastic controllers outperformed the PD. The effect of the controller became negligible for the high damping case.

The low damping case gave the best speed scores and the high damping gave the worst, which was opposite of the accuracy results as expected. Fig 10(c) shows that the compensating system provided a compromise. The SLQR and baseline gave similar results, but were both better performing than the LQG.

The results confirm the initial hypothesis that the compensating system would outperform the current state-of-the-art. The stochastically tolerant controllers yielded better accuracy than the baseline PD, with the SLQR controller excelling in the speed task. This supports implementation of such an SLQR controller in a stiffness compensating system.

VI. Conclusion

A methodology for controlling a coupled human-robot system that could account for the stochastic variation of human dymanic characteristics was presented and integrated into an existing stiffness compensating controller. In testing, compensating controller was confirmed to be effective at providing both stability and performance. The stochastic system gave improved accuracy, with the SLQR achieving this without sacrificing speed, demonstrating improvements over the previously presented system.

The system could be further enhanced with a more advanced operator model. The threshold system has several disadvantages, while a probabilistic model could likely acieve better results. The authors are currently developing a Hidden Markov Model based method that will provide better operator action estimates. Numerous controller enhancements, including closing the force loop on the impedance controller, are also being considered. These will ultimately enable testing on a device with more degrees of freedom.

VII. Acknowledgements

The authors acknowledge General Motors, the National Science Foundation (IIS EAGER 1142438, CNS 1059362), and the Center for Robotics and Intelligent Machines at Georgia Tech for sponsorship. Also, thanks to Timothy McPherson of the Bio-Robotics & Human Modeling Lab, JD Huggins of the Intelligent Machine Dynamics Lab, Dr. Minoru Shinohara of the Applied Physiology Department, and Dr. Karen Feigh of the Cognitive Engineering Center at Georgia Tech for assistance and advice.

References

[1] H. Kazerooni and M.-G. Her, "The dynamics and control of a haptic interface device," *Trans on Rob and Automation*, vol. 10, no. 4, pp. 453–464, 1994.

[2] H. Kazerooni, A. Chu, and R. Steger, "That Which Does Not Stabilize, Will Only Make Us Stronger," *Intl J of Rob Res*, vol. 26, no. 1, pp. 75–89, 2007.

[3] P. Y. Li, "Design and Cont of a Hydraulic human power amplifier," in *Intl Mech Eng Cong and Expo*, (Anaheim, CA, USA), pp. 385–393, 2004.

[4] B. Siciliano and L. Villani, *Robot force control*. Kluwer international series in engineering and computer science, Kluwer Academic, 1999.

[5] N. Hogan, "Controlling impedance at the man/machine interface," in *Intl Conf on Rob and Automation*, (Scottsdale, AZ, USA), pp. 1626–1631, Comput. Soc. Press, 1989.

[6] M. Zinn, B. Roth, O. Khatib, and J. K. Salisbury, "A New Actuation Approach for Human Friendly Robot Design," *The Intl J of Rob Res*, vol. 23, no. 4, pp. 379–398, 2004.

[7] D. W. Franklin, R. Osu, E. Burdet, M. Kawato, and T. E. Milner, "Adaptation to stable and unstable dynamics achieved by combined impedance control and inverse dynamics model.," *J of Neruophys*, vol. 90, no. 5, pp. 3270–82, 2003.

[8] M. D. Hill and G. Niemeyer, "Real-time estimation of human impedance for haptic interfaces," in *Joint Eurohaptics Conf and Symp on Haptic Interfaces for Virtual Env and Teleoperator Systems*, (Salt Lake City, UT, USA), pp. 440–445, IEEE, 2009.

[9] F. Mobasser and K. Hashtrudi-Zaad, "Adaptive Teleoperation Cont using Online Estimate of Operator's Arm Damping," in *Conf on Dec and Cont*, (San Diego, CA, USA), pp. 2032–2038, Ieee, 2006.

[10] A. V. Hill, "The heat of shortening and the dynamic constants of muscle," *Proceedings of the Royal Society of London. Series B, Biolog Sciences*, vol. 126, no. 843, pp. 136–195, 1938.

[11] N. A. Bernstein, *The co-ordination and regulation of movements*. Pergamon Press, 1967.

[12] J. A. Monroy, A. K. Lappin, and K. C. Nishikawa, "Elastic Properties of Active Muscle - On the Rebound?," *Exercise and Sport Sciences Revs*, vol. 35, no. 4, pp. 174–179, 2007.

[13] T. Sinkjæ r and R. Hayashi, "Regulation of wrist stiffness by the stretch reflex.," *J of Biomechanics*, vol. 22, no. 11-12, pp. 1133–40, 1989.

[14] N. Hogan, "Adaptive control of mechanical impedance by coactivation of antagonist muscles," *Trans on Auto Cont*, vol. 29, no. 8, pp. 681–690, 1984.

[15] E. J. Perreault, R. F. Kirsch, and P. E. Crago, "Voluntary Cont of Static Endpoint Stiffness During Force Regulation Tasks," *J of Neruophys*, vol. 87, no. 6, pp. 2808–2816, 2002.

[16] F. E. Zajac, "Muscle and tendon: Properties, models, scaling, and application to biomechanics and motor control," *Crit Revs in Biomed Eng*, vol. 17, no. 4, pp. 359–411, 1989.

[17] K. P. Tee, E. Burdet, C. M. Chew, and T. E. Milner, "A model of force and impedance in human arm movements," *Biolog Cybernetics*, vol. 90, no. 5, pp. 368–375, 2004.

[18] E. Burdet, R. Osu, D. W. Franklin, T. E. Milner, and M. Kawato, "The central nervous system stabilizes unstable dynamics by learning optimal impedance.," *Nature*, vol. 414, no. 6862, pp. 446–9, 2001.

[19] D. W. Franklin and T. E. Milner, "Adaptive control of stiffness to stabilize hand position with large loads.," *Exp Brain Res*, vol. 152, no. 2, pp. 211–220, 2003.

[20] W. Gallagher, T. McPherson, J. D. Huggins, M. Shinohara, D. Gao, R. Menassa, and J. Ueda, "An Improved Human-Robot Interface by Measurement of Muscle Stiffness," in *Intl Conf on Biomed Rob and Biomecha*, (Rome, Italy), 2012.

[21] W. Gallagher, D. Gao, and J. Ueda, "Measurement of muscle stiffness to improve stability of haptic human-robot interfaces," in *Dynamic Systems and Cont Conf*, (Ft. Lauderdale, FL, USA), 2012.

[22] W. Gallagher, D. Gao, and J. Ueda, "Improved Stability of Haptic Human-Robot Interfaces using Measurement of Human Arm Stiffness," *Adv Rob*, 2014.

[23] W. Gallagher, M. Ding, and J. Ueda, "Relaxed individual control of skeletal muscle forces via physical human-robot interaction," *Multibody Sys Dyn*, vol. 30, no. 1, pp. 77–99, 2013.

[24] K. Zhou, J. C. Doyle, and K. Glover, *Robust and Opt Cont*. Prentice Hall, 1996.

[25] W. L. De Koning, "Infinite horizon optimal control of linear discrete time systems with stochastic parameters," *Automatica*, vol. 18, no. 4, pp. 443–453, 1982.

[26] R. E. Kalman, "A new approach to linear filtering and prediction problems," *J of Basic Eng*, vol. 82, no. 1, pp. 35–45, 1960.

[27] M. Athans, "The role and use of the stochastic linear-quadratic-Gaussian problem in control system design," *Trans on Auto Cont*, vol. 16, no. 6, pp. 529–552, 1971.

[28] E. Yaz, "Minimax control of discrete nonlinear stochastic systems with noise uncertainty," in *Conf on Dec and Cont*, (Brighton, England, UK), pp. 1815–1816, 1991.

[29] M. Kárný and T. V. Guy, "Fully probabilistic control design," *Systems & Cont Letters*, vol. 55, no. 4, pp. 259–265, 2006.

[30] Z. Wang, D. W. C. Ho, Y. Liu, and X. Liu, "Robust control for a class of nonlinear discrete time-delay stochastic systems with missing measurements," *Automatica*, vol. 45, no. 3, pp. 684–691, 2009.

[31] K. Fujimoto, S. Ogawa, Y. Ota, and M. Nakayama, "Opt control of linear systems with stochastic parameters for variance suppression: The finite time horizon case," in *IFAC World Cong*, (Milan, Italy), pp. 12605–12610, 2011.

[32] K. Fujimoto, Y. Ota, and M. Nakayama, "Opt control of linear systems with stochastic parameters for variance suppression," in *Conf on Dec and Cont and European Cont Conf*, (Orlando, FL, USA), pp. 1424–1429, Ieee, 2011.